Hierarchical Energy Management System for Home-Energy-Hubs Considering Plug-in Electric Vehicles

Hamid Reza Gholinejad, Jafar Adabi, Mousa Marzband, *Senior Member, IEEE*

***Abstract*—The escalating demand on Electric Vehicles (EVs) has enhanced the necessity of adequate charging infrastructure, especially in residential areas. This paper proposes a smart charging approach for off-board Electric Vehicles (EVs) chargers in Home-Energy-Hub (HEH) applications along with DC sources such as Photovoltaic (PV) and Battery Storage (BS). The proposed method facilitates smart charging and discharging of EVs to obtain both Vehicle-to-X (V2X) and X-to-Vehicle (X2V) operations focusing on the domestic applications integrated with renewable and storage elements. Furthermore, the optimal State-of-Charge (SOC) profiles for BS and EV in the HEHs system is defined by the extended Bellman-Ford-Moor Algorithm (BFMA). This modified BFMA utilizes the forecasted data such as solar irradiation, electricity tariff, and power consumption to gain economic benefits in HEHs with respect to user and EV requirements. Moreover, the plugging time, duration and initial/final SOC are fluctuating at each connection due to the stochastic nature of EV conditions and user settings. This study presents a laboratory implementation of two-level Hierarchical Energy Management System (HEMS) for HEHs with plug-in electric vehicles. In fact, the primary level includes power converters controller, while the proposed algorithm is implemented in the secondary level. Finally, the simulation and experimental results confirm the effectiveness of the proposed analysis regarding the interaction of HEHs and power grid with EVs behavior.**

***Index Terms*—Hierarchical energy management system; Home-energy-hub; Electric vehicle; Vehicle-to-Grid; Smart charging and discharging.**

NOMENCLATURE

Abbreviation

BS	Battery storage
$BFMA$	Bellman-Ford-Moor algorithm
CC	Constant Current
CCB	Current control board
CV	Constant voltage
DP	Dynamic programming
EV	Electric vehicle
EMS	Energy management system
$HEMS$	Hierarchical energy management system
HEH	Home-Energy-Hub
$MILP$	Mixed integer linear programming
PLL	Phase-locked loop
PV	Photovoltaic
RCC	Reduced constant current
PI	Proportional-Integral
RES	Renewable Energy Source
SOC	State-of-Charge
$V2G$	Vehicle-to-Grid
$V2X$	Vehicle-to-X
$X2V$	X-to-Vehicle
X	Home, Grid, Vehicle, $\cdots$

Indices

g, t, ev	Indices of power grid, time-step, electric vehicle
j, k	Indices of SOC at two consecutive time-steps

Parameters

$i_L^{BS}, i_L^{\text{EV}}, i_L^{\text{PV}}$	Inductor currents of BS, EV, and PV
i_g, i_{gd}^*, i_{gq}^*	Instantaneous, and references value of d-axis and q-axis currents of power grid
v_g, v_{gd}, v_{gq}	Instantaneous, d-axis and q-axis voltage of power grid
$P_{\text{Charge}}^{\text{BS}\|\|\text{EV}}, P_{\text{Discharge}}^{\text{BS}\|\|\text{EV}}$	Maximum charge and discharge power of the batteries
L_g, ω_g, θ_g	L-filter, angular frequency and phase of power grid
v_{dc}, $v_{dc}^\star$, $Q^\star$, P_{ref}^{PV}	Instantaneous and references value of DC bus voltage, and reference of power grid reactive power and PV power
n, n_{ev}	Number of nodes per time-step
t_0, t_{Target}	Start and stop times BS scheduling
$t_{in}^{\text{EV}}, t_{out}^{\text{EV}}$	Connection and disconnection times of EV
$\text{SOC}_t^{\text{BS},k}$	k^{th} BS SOC of time-step t
$\text{SOC}_{t+\Delta t}^{\text{BS},j}$	j^{th} SOC of time-step $(t+\Delta t)$
$\text{SOC}_{t_0}^{\text{BS}}$, $\text{SOC}_{t_{\text{Target}}}^{\text{BS}}$	Initial and target SOCs of BS
$\text{SOC}_{t_{in}}^{\text{EV}}$, $\text{SOC}_{t_{out}}^{\text{EV}}$	Initial and target SOCs of EV
$\text{SOC}_t^{\text{BS},max}$, $\text{SOC}_t^{\text{BS},min}$	Upper and lower limit of BS SOC
$\text{SOC}_t^{\text{EV},max}$, $\text{SOC}_t^{\text{EV},min}$	Upper and lower limit of EV SOC
$\Delta\text{SOC}_{(t,t+\Delta t)}^{\text{BS},(k,j)}$, $\Delta\text{SOC}_{(t,t+\Delta t)}^{\text{EV},(k,j)}$	Changes of BS and EV SOCs when crosses from node k of time-step t to node j of time-step $(t+\Delta t)$
$\Delta P_{(t,t+\Delta t)}^{\text{BS},(k,j)}$, $\Delta P_{(t,t+\Delta t)}^{\text{EV},(k,j)}$, $\Delta P_{(t,t+\Delta t)}^{\text{HEH},(k,j)}$	Changes of BS, EV, and HEH powers when crosses from node k of time-step t to node j of time-step $(t+\Delta t)$

The work is supported by the British Council under grant contract No: IND/CONT/GA/18-19/22.

Hamid Reza. Gholinejad and Jafar Adabi are with faculty of Electrical and Computer Engineering, Babol Noshirvani University of Technology, Babol, Iran. (email: ffamid.reza@gmail.com, j.adabi@nit.ac.ir)

Mousa Marzband is with Faculty of Engineering and Environment, Northumbria University, Newcastle upon Tyne NE1 8ST, UK and also with center of research excellence in renewable energy and power systems, King Abdulaziz University, Jeddah, Saudi Arabia (email: mousa.marzband@northumbria.ac.uk).

$\delta\text{SOC}_t^{\text{BS}}$, $\delta\text{SOC}_t^{\text{EV}}$	Step size of BS and EV SOC
C_{AH}^{BS}, V^{BS}	Battery capacity and battery voltage of BS
C_{AH}^{EV}, V^{EV}	Battery capacity and battery voltage of EV
$W_{(t,t+\Delta t)}^{(k,j)}$	Cost function value when crosses from node k of time-step t to node j of time-step $(t+\Delta t)$
Γ	Electricity tariff

I. Introduction

GROWING demand of plug-in EVs introduces new types of loads in power systems. Despite the environmental benefits, EVs contain stochastic charging demand and impose additional load on power grid [1]. Various charging rates, initial SOC, and plug-in time are the factors causing stochastic behavior of EVs [2]. Forming home-scaled energy systems with real-time multi-objective Energy Management System (EMS) could be interesting solutions to these challenges. In fact, the HEH is identified as an integration of a variety of small-scale energy generators, energy converters, and energy storage units causing to reduce dependency on power plants and enhance utilization of Renewable Energy Sources (RES) [3]. Further, the most suitable EMS structure for the integrated energy systems is hierarchical architecture [4]. Extensive communication and maximum level of coordination hinder implementation of fully centralized and decentralized control structures [5]. In fact, the hierarchical architectures compromise among other control structures. The couple of works of literature dealing with the same subject are explained in details below.

Optimal scheduling of an energy hub including energy storage system and integrated EV is investigated in [6]. A mixed integer linear programming (MILP) optimization to manage the domestic peak load demand for home-scaled prosumers including PV, BS, and EV is presented in [7]. However, performance of the proposed approach has not been validated experimentally. Further, a novel and effective charging method to deal with charging pattern for residential EVs is introduced in [8]. Nevertheless, the method has considered only EV charging load pattern, and V2G operation mode has been ignored. A novel home EMS is presented in [9] considering energy price and PV power generation uncertainties along with maximizing plug-in EV battery life span. Predominantly, home EMSs has been verified from a simulation perspective, while practical implementation identifies the key deviations from simulation results. A multi-functional EV charger is implemented practically in a grid-connected PV-based home microgrid in [10]. A novel state-space approximate Dynamic Programming (DP) approach for fast real-time decision-making in home EMS is proposed in [11]. The optimal routing of EVs' SOC is discussed in [12]. In this respect, the shortest path is discovered considering limited battery capacity to minimize the charging times. However, none of the above studies have considered the stochastic behavior of EVs such as random connecting time, different plugged-in duration, and different initial and target SOC.

An effective charging/ discharging method is suggested in [13] where the experimental results have proved that the proposed method could significantly reduce the energy cost and energy dependency on the power grid. Furthermore, a charging/ discharging framework for EVs for effective utilization of PV is proposed in [14]. A comprehensive independent energy system and cost-effective charging would be achieved by a multi-energy system considering the BS optimal charging and discharging. Moreover, the real-time pricing to compute the BS system schedule is considered in [15], where the EV has accounted for an uncertain load. An efficient EMS for an integrated system with PV, BS, and EV to facilitate EV and BS charging is proposed in [16]. Although the unexpected peak power demand and the V2G implementation is controlled by the EMS, this method failed to address the electricity tariff, as EMS is SOC-based. Hence, the BS and EV are charged even during the high electricity tariff periods, which is not cost effective. This requires a comprehensive observation of the multi-energy system, and hierarchical structure is one of the best candidates in this regard. Moreover, a charging and discharging strategy for both the BS and EV for economic energy modeling in home applications are proposed in [16]. In fact, the model derives a user-friendly energy scheduling framework for the smart home, resulting the lowest energy cost. However, these schemes utilize complex calculations to evaluate the optimal solutions. A home EMS strategy to coordinate the charging/ discharging operation of the multi-trip EVs is proposed in [17], which deals with the various charging and discharging situations. Nonetheless, this strategy is only suitable for the scenarios with lack of RESs and BSs.

Consequently, the literature works on home EMS and EV charging could be classified into different major categories of (a) optimality, multi-energy systems, and (c) uncertainty consideration. Among these works, insignificant number of papers has addressed all three categories as well as power converters control in real-time experimental tests. Table I compares a number of papers from this perspective. This table has also presented the advantages and disadvantages of the most interesting methods in home EMS and EV charging. This study has concentrated on the power converters control based on a two-level (primary and secondary) HEMS architecture for HEHs considering the stochastic behavior of EVs. The main contributions of the proposed strategy could be identified as:

- A two-level HEMS for multi-energy systems is designed to manage and achieve pre-defined user objectives with simple implementation.
- An optimization algorithm based on the day-ahead and the instantaneous data to make fast real-time decisions under the stochastic behavior of EV.
- Satisfactory results in terms of target SOC attainment, financial benefits, and avoiding batteries overcharging/ over-discharging can be achieved.
- System uncertainties and charging modes such as constant current (CC) and reduced constant current (RCC) are considered.

The remaining parts of the paper are organized as below. Section II gives an overview of the system. Section III

TABLE I: Comparison of different algorithm in the literature

Method	Ref	Stochastic EV	Power converter switching	Classification	Pros	Cons
Mixed-integer linear programming (MILP)	[18], [19]	✓	x	(a)	Flexible and powerful for solving large and complex problems	Non-linear effects cannot be taken into account, need to consider the whole-time horizon at once
	[20]	x	✓	(a), (b)		
Particle Swarm Optimization (PSO)	[21]	x	✓	(a), (b)	Easy hardware implementation, strong global search capability, fast convergence speed, and less computational complexity	Relatively high computational time, unsuitable for real-time applications
	[22]	x	x	(a), (b), (c)		
Model Predictive Control (MPC)	[23]	x	✓	—	Robust against uncertainty, multiple control objective can be implemented for the same control strategy	Computational complexity, highly dependent to control parameters information
	[24]	✓	x	(a), (c)		
Heuristic optimizations	[25]	✓	x	(a), (b)	Offers a quick solution, easy to understand and implementation, practical	Unable to assure optimally of the obtained results
	[26], [27]	x	x	(a), (b)		
Stochastic programming	[28], [29]	✓	x	(a), (b), (c)	Provide convenient tools to model uncertainties	Complexity of large multi-stage stochastic problems
	[30]–[32]	x	x	(a), (b), (c)		
Rule-based	[33], [34]	x	x	(a), (b)	Simple structure, high reliability, and practical	Unable to deal with large data
	[35]	x	x	(a), (b), (c)		
Artificial neural network (ANN)	[36]	✓	x	(a), (c)	Fast solution for problems in control and prediction	Complex design and implementation, requires learning process
	[37], [38]	x	x	(b)		
Fuzzy logic control (FLC)	[39]	x	x	(b)	Simple structure, Easy design and implementation, and handle nonlinear systems	Depends on appropriate rule-based algorithms and membership functions which are commonly determined on the basis of trial and error
	[40]	x	x	—		
Adaptive neural fuzzy inference system (ANFIS)	[41]	x	x	(b)	Ability to capture the nonlinear structure of a process, adaptation capability, and rapid learning capacity	Large amount of data required and long training and learning times
	[42]	x	x	(b)		
DP	[43]	x	x	(a), (b)	Optimal decision capability, proper to solve more complex problems	Require future data profile to make a decision, difficult to implement in embedded devises
	[44]	x	x	(a), (b), (c)		
	Proposed method	✓	✓	(a), (b), (c)		

discusses the proposed two-level HEMS. Section IV presents the simulation and experimental results of various case studies. The paper ends with conclusions in Section V.

II. System description

HEH is equipped with DC source, BS, and EV in this study. According to Fig. 1, each device is connected to a common DC bus via the individual DC-DC converters. A single-phase bidirectional DC/AC converter performs as an interface between the DC bus and the power grid. The proposed HEMS consists of two primary and secondary levels. The primary level generates the switching pulse following the secondary level references. This level includes measurements and control system to regulate the voltage and currents based on the determined power references by the secondary level. In the primary level, each DC-DC converter is controlled as a current source with PI controller. The current reference of parallel DC-DC converters is determined by the secondary level. In particular,, the secondary level acts as a Central Control Board (CCB) which determines the current reference of each converter. In fact, the CCB divides the measured load current by the number of parallel DC-DC converters [45]. In the proposed method, the reference currents are determined according to a multi-objective optimization algorithm. The single-phase bidirectional DC/AC converter is also controlled as a current source, which current reference is determined by the DC bus voltage error. In this regard, the DC bus voltage is measured to set the current amplitude on AC side [46]. Further, the grid voltage phase, frequency, and amplitude are extracted by the phase-locked loop (PLL). In the secondary level, BFMA is deployed as a popular DP algorithm to adapt the HEMS with the stochastic behavior of the EV. As illustrated in Fig. 1, the forecast data (solar irradiance, load demand) and the measured quantities (batteries' SOC) are considered as the input data for the secondary level. This structure could be extended by considering a couple of neighboring HEHs to achieve a large-scale integration of RESs, BSs, and EVs. A detailed description of the proposed secondary level is presented in the next section.

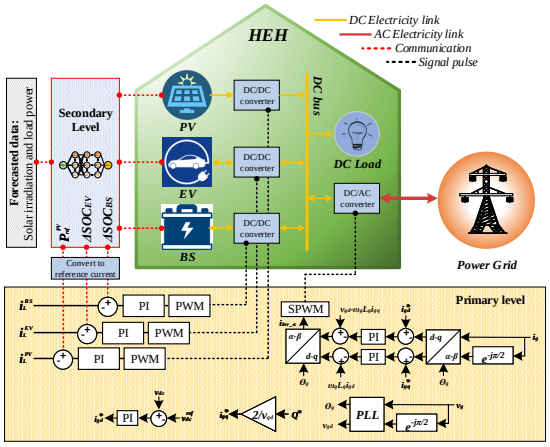

Fig. 1: System structure

III. Proposed two-level HEMS

As mentioned above, the secondary level input data is determined by the forecast data, user settings and the measured quantities. The outputs are optimal charge/ discharge profiles of BS and plugged-in EV. The power sharing of the system is determined to achieve the optimal SOCs. The system continues its operation, even if the EV is disconnected. When the EV is reconnected, the optimal profile of SOCs should be determined again based on the new EV status for remained time-steps of the day. Therefore, the optimization algorithm should be relatively fast for real-time implementation process. BFMA is an optimization technique which utilizes to find the shortest path through a graph [11], [12]. This method breaks up the complex energy management problems into a series of sub-problems to speed up the process for real-time decisions [11]. In the following sections, the principles of conventional BFMA and modified BFMA are described, respectively.

A. Conventional BFMA

As shown in Fig. 2, the BS charging problem is divided into a multi-stage decision process. At each time, t, a set of SOC states, $SOC_t^{\mathrm{BS,k}}$, is estimated, and discretized with steps (k=1,$\cdots$,n).$\mathrm{SOC}_t^{\mathrm{BS,max}}$, $SOC_t^{\mathrm{BS,min}}$, and $\delta SOC_t^{\mathrm{BS}}$ are the upper limit, lower limit and the step size of SOC, respectively [47]. The goal is to find the shortest path between the $SOC_{t_0}^{\mathrm{BS}}$ and $SOC_{t_{\mathrm{Target}}}^{\mathrm{BS}}$ by crossing all possible sets of SOC states. t0 and t_{Target} are the start and stop time of algorithm, respectively.

Each change of SOC states from $SOC_t^{\mathrm{BS,k}}$ to $SOC_{t+\Delta t}^{\mathrm{BS,j}}$, (j=1,$\cdots$,k,$\cdots$,n), represents an edge $\mathrm{E}(\Delta SOC_t^{\mathrm{BS,k}}, \Delta SOC_{t+\Delta t}^{\mathrm{BS,j}})$ in the graph of Fig. 2. Crossing an edge leads to charge or discharge of the BS, which corresponding power is obtained by Eq. (1).

$$\Delta P_{(t,t+\Delta t)}^{\mathrm{BS,(k,j)}} = \Delta SOC_{(t,t+\Delta t)}^{\mathrm{BS,(k,j)}} C_{AH}^{\mathrm{BS}} V^{\mathrm{BS}} \tag{1}$$

where, C_{AH}^{BS}, and V^{BS} are the BS capacity and voltage, respectively. Further, SOC change through crossing the edge is as Eq. (2).

$$\Delta SOC_{(t,t+\Delta t)}^{\mathrm{BS,(k,j)}} = \mathrm{SOC}_t^{\mathrm{BS,k}} - \mathrm{SOC}_{(t+\Delta t)}^{\mathrm{BS,j}} \tag{2}$$

If $\Delta SOC_{(t,t+\Delta t)}^{\mathrm{BS,(k,j)}} > 0$ and $\Delta SOC_{(t,t+\Delta t)}^{\mathrm{BS,(k,j)}} < 0$, the BS is discharged and charged, respectively. By determining $\Delta P_{(t,t+\Delta t)}^{\mathrm{BS,(k,j)}}$, power excess/shortage could be

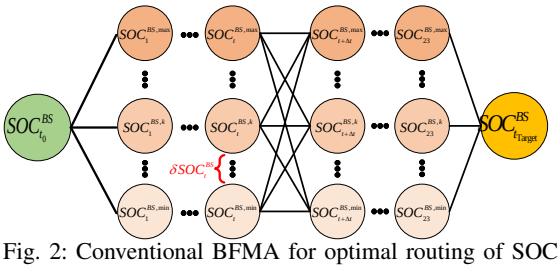

Fig. 2: Conventional BFMA for optimal routing of SOC

obtained according to the day-ahead PV and load power as Eq. (3).

$$\Delta P_{(t,t+\Delta t)}^{\mathrm{HEH},(k,j)} = \left(\begin{array}{l} P_{t+\Delta t}^{\mathrm{PV}} - P_{t+\Delta t}^{LOAD} \\ +\Delta P_{(t,t+\Delta t)}^{BS,(k,j)} \end{array} \right) \Bigg|_{\substack{t=t_0,\cdots,t_{T\arg et} \\ k=1,\cdots,n \\ j=1,\cdots,n}} \tag{3}$$

To find the shortest path, the financial profit is considered as the weight of each edge $W_{(t+\Delta t)}^{(k,j)}$. Therefore, this parameter is calculated according to the $\Delta P_{(t,t+\Delta t)}^{\mathrm{HEH},(k,j)}$ and electricity tariff, $\Gamma_{(t+\Delta t)}$. According, to the pseudo-code shown in Algorithm 1, the BFMA searches for the shortest path, which indicates the amount of BS' SOC between t_0 and t_{Target}.

Algorithm 1 BFMA

Require: Initialization ▷ Hourly prediction data of HEH, $\mathrm{SOC}_{t_0}^{\mathrm{BS}}$, $\mathrm{SOC}_{t_{\mathrm{Target}}}^{\mathrm{BS}}$, $\mathrm{SOC}_{t_{\mathrm{in}}}^{\mathrm{EV}}$, $\mathrm{SOC}_{t_{\mathrm{out}}}^{\mathrm{EV}}$, $\delta\mathrm{SOC}_t^{\mathrm{BS}}$, $\delta\mathrm{SOC}_t^{\mathrm{EV}}$, $\mathrm{SOC}_t^{\mathrm{BS,max}}$, $\mathrm{SOC}_t^{\mathrm{BS,min}}$, $\mathrm{SOC}_t^{\mathrm{EV,max}}$, $\mathrm{SOC}_t^{\mathrm{EV,min}}$, $P_{\mathrm{Charge}}^{\mathrm{BS||EV}}$, $P_{\mathrm{Discharge}}^{\mathrm{BS||EV}}$, and Γ_t.

$$D\left(\mathrm{SOC}_t^{\mathrm{BS},k}\right) \leftarrow \infty, \quad \forall t \neq t_0 \tag{4}$$

▷ **Set initial distance**

$$D\left(\mathrm{SOC}_{t_0}^{\mathrm{BS}}\right) \leftarrow 0, \quad \forall t = t_0 \tag{5}$$

▷ **Distance to start node**

for t= t_0: t_{Target} **do**
  for k= 1: n **do**
    for j= 1: n **do**

$$W_{(t+\Delta t)}^{(k,j)} = \frac{1}{\left(\Delta P_{(t,t+\Delta t)}^{\mathrm{HEH},(k,j)} \times \Gamma_{(t+\Delta t)}\right)}; \quad \Delta P_{(t,t+\Delta t)}^{\mathrm{HEH},(k,j)} > 0 \tag{6}$$

$$W_{(t+\Delta t)}^{(k,j)} = \Delta P_{(t,t+\Delta t)}^{\mathrm{HEH},(k,j)} \times \Gamma_{(t+\Delta t)}; \quad \Delta P_{(t,t+\Delta t)}^{\mathrm{HEH},(k,j)} < 0 \tag{7}$$

$$D\left(\mathrm{SOC}_t^{\mathrm{BS},j}\right) = min[D\left(\mathrm{SOC}_{t+\Delta t}^{\mathrm{BS},j}\right), D\left(\mathrm{SOC}_t^{\mathrm{BS},k}\right) + W_{(t+\Delta t)}^{(k,j)}] \tag{8}$$

    end for
  end for
end for
  return Return determine the optimum SOC profile of BS and EV.

As seen before, the conventional BFMA properly provides the optimal profile of SOC changes, which could effectively be used in optimal charge and discharge management of BS in HEH. However, if one or more plugged-in EVs are available and two or more optimal profiles should be determined, it cannot be applicable anymore. In the next subsection, a modification of BFMA is discussed in order to present (or evaluate) the scalability of the two or more optimal profiles.

B. Modified BFMA

In this section, in order to achieve two or more optimal profiles, the conventional BFMA has slightly been changed, which does not impose mathematical complexity and is suitable for applications with several optimal charging and discharging units. Assume that EV is connected at t_{in}^{EV} (stochastically) with $\mathrm{SOC}_{t_{in}}^{\mathrm{EV}}$ (measured). The EV owner should set two parameters: (1) unplug time (t_{out}^{EV}) and (2) $\mathrm{SOC}_{t_{out}}^{\mathrm{EV}}$ to make EV charge and discharge optimal. Prior to connecting EV, the system operates on conventional BFMA results. By EV plugging, SOC measuring and setting the two

aforementioned parameters, the modified BFMA will run.

Fig. 3 shows the scheme of the proposed BFMA with a plugged-in EV. Brighter blue and brown semicircles indicate lower SOC states of EV and BS, respectively. Similarly, the green and yellow semicircles are the initial and target SOCs of EV, respectively. In this regard, the number of SOC states (nodes), at the time-steps that the EV is connected except t_{in}^{EV} and t_{out}^{EV}, is changed. As shown in this figure, for a given SOC state of BS at each time-step, there would be several SOC states for EV. In other words, considering the number of SOC states of EV, $n_{ev} = \left(\mathrm{SOC}_t^{EV,\max} - \mathrm{SOC}_t^{EV,\min}\right) \Big/ \delta\mathrm{SOC}_t^{EV}$, $(t = t_{in}^{\mathrm{EV}} + 1, \cdots, t_{out}^{\mathrm{EV}} - 1)$, there will be n_{ev}, there will be n_{ev} states for EV per SOC states of the BS. Hence, the total number of nodes will be $n \times n_{ev}$ while an EV is connected.

As the number of nodes increases, the more computational time would be needed. However, it should be noted that by crossing each possible path, many SOC states would be eliminated because of the constraints. The $\Delta\mathrm{SOC}_{(t,t+\Delta t)}^{BS,(k,j)}$ and $\Delta\mathrm{SOC}_{(t,t+\Delta t)}^{EV,(k,j)}$ are not allowed to be greater than the certain amount during a time-step because of the nominal power of charger and the specifications of the batteries.

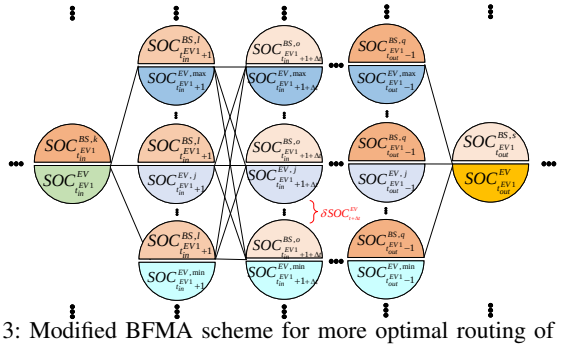

Fig. 3: Modified BFMA scheme for more optimal routing of SOCs

Here, crossing an edge may lead to charge or discharge of the both BS and EV, simultaneously. Hence, the corresponding power is obtained from Eq. (9).

$$\Delta P_{(t,t+\Delta t)}^{\mathrm{HEH},(k,j)} = \left(\begin{array}{l} P_{t+\Delta t}^{\mathrm{PV}} - P_{t+\Delta t}^{LOAD} \\ +\Delta P_{(t,t+\Delta t)}^{BS,(k,j)} \\ +\Delta P_{(t,t+\Delta t)}^{EV,(k,j)} \end{array} \right) \Bigg|_{\substack{t=t_0,\cdots,t_{\mathrm{Target}} \\ k=1,\cdots,n \\ j=1,\cdots,n}} \tag{9}$$

where,

$$\Delta P_{(t,t+\Delta t)}^{EV,(k,j)} = \Delta\mathrm{SOC}_{(t,t+\Delta t)}^{EV,(k,j)} \times C_{AH}^{EV} \times V^{EV} \tag{10}$$

$$\Delta\mathrm{SOC}_{(t,t+\Delta t)}^{EV,(k,j)} = \mathrm{SOC}_t^{EV,k} - \mathrm{SOC}_{t+\Delta t}^{EV,j} \tag{11}$$

C_{AH}^{EV} and V^{EV} are the EV capacity and voltage, respectively. The conventional BFMA pseudo-code will be modified as shown in Algorithm 2. The nodes range at different time-steps are changed after the EV connection.

C. Constraints

In order to prevent the increasing time for the charge/ discharge scheduling of multiple EVs, the problem is restricted to the maximum charge and discharge power of the batteries, $P_{Charge}^{BS||EV}$ and $P_{Discharge}^{BS||EV}$, as shown in Fig. 4. This means that at a given time-step, $\Delta\mathrm{SOC}_{(t,t+\Delta t)}^{BS||EV,(k,j)}$, would not exceed the

Algorithm 2 MODIFIED BFMA

Require: Initialization ▷ Hourly prediction data of HEH, $\mathrm{SOC}_{t_0}^{\mathrm{BS}}$, $\mathrm{SOC}_{t_{\mathrm{Target}}}^{\mathrm{BS}}$, $\mathrm{SOC}_{t_{\mathrm{in}}}^{\mathrm{EV}}$, $\mathrm{SOC}_{t_{\mathrm{out}}}^{\mathrm{EV}}$, $\delta\mathrm{SOC}_t^{\mathrm{BS}}$, $\delta\mathrm{SOC}_t^{\mathrm{EV}}$, $\mathrm{SOC}_t^{\mathrm{BS,max}}$, $\mathrm{SOC}_t^{\mathrm{BS,min}}$, $\mathrm{SOC}_t^{\mathrm{EV,max}}$, $\mathrm{SOC}_t^{\mathrm{EV,min}}$, $P_{\mathrm{Charge}}^{\mathrm{BS||EV}}$, $P_{\mathrm{Discharge}}^{\mathrm{BS||EV}}$, and Γ_t.

$$D\left(\mathrm{SOC}_{\mathrm{t}}^{\mathrm{BS},k}, \mathrm{SOC}_{\mathrm{t}}^{\mathrm{EV},k}\right) \leftarrow \infty, \quad \forall t \neq t_0 \tag{12}$$

▷ **Set initial distance**

$$D\left(\mathrm{SOC}_{t_{in}^{\mathrm{EV}}}^{\mathrm{BS}}, \mathrm{SOC}_{t_{in}^{\mathrm{EV}}}^{\mathrm{EV},k}\right) \leftarrow 0, \quad \forall t = t_0 \tag{13}$$

▷ **Distance to start node**

for t= t_{in}^{EV}: t_{Target} **do**
  if $t_{\mathrm{in}}^{\mathrm{EV}}$+1 < t < $t_{\mathrm{out}}^{\mathrm{EV}}$ **then** k_t= n × n_{ev}
  else k_t= n
  end if
  if $t_{\mathrm{in}}^{\mathrm{EV}}$ ≤ t < $t_{\mathrm{out}}^{\mathrm{EV}}$ **then** J_t= n × n_{ev}
  else if $t_{\mathrm{out}}^{\mathrm{EV}}$ ≤ t < t_{out} **then** J_t= n
  else J_t= 1
  end if
  for k= {1: n for $t = t_{in}^{\mathrm{EV}}$} **do**
    for j= 1: n **do**
Check the constraints; ▷ Refer to **Fig. 4**

$$W_{(t+\Delta t)}^{(k,j)} = \frac{1}{\left(\Delta P_{(t,t+\Delta t)}^{\mathrm{HEH},(k,j)} \times \Gamma_{(t+\Delta t)}\right)}, \quad \Delta P_{(t,t+\Delta t)}^{\mathrm{HEH},(k,j)} > 0 \tag{14}$$

$$W_{(t+\Delta t)}^{(k,j)} = \Delta P_{(t,t+\Delta t)}^{\mathrm{HEH},(k,j)} \times \Gamma_{(t+\Delta t)}, \quad \Delta P_{(t,t+\Delta t)}^{\mathrm{HEH},(k,j)} < 0 \tag{15}$$

$$D\left(\mathrm{SOC}_{t+\Delta t}^{\mathrm{BS},j}, \mathrm{SOC}_{t+\Delta t}^{\mathrm{EV},j}\right) = min[D\left(\mathrm{SOC}_{t+\Delta t}^{\mathrm{BS},j}, \mathrm{SOC}_{t+\Delta t}^{\mathrm{EV},j}\right) \tag{16}$$

$$D\left(\mathrm{SOC}_{t}^{\mathrm{BS},k}, \mathrm{SOC}_{t+\Delta t}^{\mathrm{EV},k}\right) + W_{(t+\Delta t)}^{(k,j)}] \tag{17}$$

    end for
  end for
end for
  return Determine the optimum SOC profile of BS and EV.

particular values. Therefore, the unwanted nodes are nullified and an acceleration factor is introduced. In addition, to protect the battery from damage at the higher SOCs, the battery charger should be used in constant voltage (CV) charging mode. However, the CV mode needed approximately three times longer duration compared to the CC mode. To improve the long charging time and preserve the safety feature without changing the control schematic, RCC mode proposed in [48] has been adapted to the proposed algorithm procedure. In this regards, for the SOCs greater than 80%, $\mathrm{P}_{Charge}^{BS||EV}$ would be decreased. To do this, at the edges ending to $SOCs > 80\%$, if the $\Delta SOCs \leq -10\%$, the edges' weigh will be infinite. As a result, some other nodes would be nullified and the maximum change of SOCs in charging mode would be more restricted during a time-step. Thus, the results presented in the Section III are based on the RCC mode. This way, the proposed method guarantees the achieving to the target SOC of BS and EVs, optimal management of RES power and maximum financial profit of HEH as well as power grid peak shaving. These incentives motivate customers and power grid to adopt and financially support such a strategy, respectively.

IV. SIMULATION AND EXPERIMENTAL RESULTS

The performance of the proposed algorithm has been investigated through the simulation and experimental results. Detailed features and results assessment are presented below.

A. Simulation

According to Fig. 1, a HEH has been simulated on MATLAB/ Simulink environment with the specifications given in Table II. The simulation results are obtained based on four following case studies (CS).

1) CS1: EV is not connected, t_0= 00:00, t_{Target}= 24:00, $\mathrm{SOC}_0^{\mathrm{BS}}$= 40%, and $\mathrm{SOC}_{\mathrm{Target}}^{\mathrm{BS}}$= 90%.

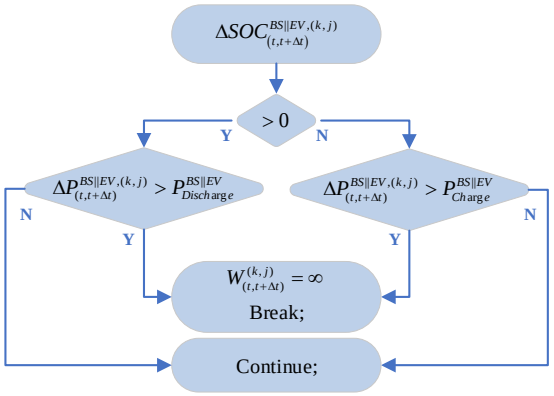

Fig. 4: Nullifying the unwanted nodes

2) CS2: EV is connected under two scenarios CS2S1 and CS2S2 which model the stochastic behavior of the EV at two connection time-steps as follows. BS parameters of BS for both CS2S1 and CS2S2 are as the same as CS1. EV parameters are also randomly considered, as described in next paragraphs.
   a) CS2S1: $t^{\text{EV}}_{\text{in1}}$= 05:00, $t^{\text{EV}}_{\text{out1}}$= 10:00, $\text{SOC}^{\text{EV}}_{t_{\text{in1}}}$= 35%, and $\text{SOC}^{\text{EV}}_{t_{\text{out1}}}$= 60%
   b) CS2S2: $t^{\text{EV}}_{\text{in2}}$= 13:00, $t^{\text{EV}}_{\text{out2}}$= 18:00, $\text{SOC}^{\text{EV}}_{t_{\text{in2}}}$= 20%, and $\text{SOC}^{\text{EV}}_{t_{\text{out2}}}$= 55%
3) CS3: EV is connected under two scenarios CS3S1 and CS3S2 which study impacts of EV disconnection before the mutually agreed upon $t^{\text{EV}}_{\text{out}}$ on SOCs optimum scheduling. BS parameters of BS for both CS3S1 and CS3S2 are the same as CS1. EV parameters are also randomly considered, as described in next paragraphs.
   a) CS3S1: $t^{\text{EV}}_{\text{in1}}$= 10:00, $t^{\text{EV}}_{\text{out1}}$= 23:00, $\text{SOC}^{\text{EV}}_{t_{\text{in1}}}$= 40%, and $\text{SOC}^{\text{EV}}_{t_{\text{out1}}}$= 85%
   b) CS3S2: $t^{\text{EV}}_{\text{in1}}$= 10:00, $t^{\text{EV}}_{\text{out2}}$= 18:00, $\text{SOC}^{\text{EV}}_{t_{\text{in1}}}$= 40%, and $\text{SOC}^{\text{EV}}_{t_{\text{out2}}}$= 65%
4) CS4: EV is connected in the case of considering load uncertainty. The BS parameters are the same as CS1, and EV parameters are manually chosen specially for CS4 as $t^{\text{EV}}_{\text{in}}$= 00:00, $t^{\text{EV}}_{\text{out}}$= 24:00, $\text{SOC}^{\text{EV}}_{t_{\text{in}}}$= 20%, and $\text{SOC}^{\text{EV}}_{t_{\text{out}}}$= 90%.
   a) CS4S1: without considering load uncertainty
   b) CS4S2: With considering load uncertainty

Fig. 5 illustrates the SOC of BS and EV according to the CS1, CS2S1, and CS2S2. This figure shows the effect of random re-connection of the EV on BS charge/ discharge scheduling. EV parameters including the connecting/ disconnecting time-steps, initial SOC and target SOC are determined randomly at the plugging time-step in the ranges of Eq. (18) to Eq. (9). Hence, stochastic behavior of EV could be modeled.

TABLE II: Simulation specifications

Description	Value	Unit
DC bus voltage	400	V
RMS voltage of power grid	230	V
BS and EV voltage	228, 114	V
BS and EV capacity	136, 102	Ah
PV maximum power and voltage	5450, 288	W, V
$\text{SOC}^{\text{BS,min}}_t$, $\text{SOC}^{\text{BS,max}}_t$, $\delta\text{SOC}^{\text{BS}}_t$	20, 90, 5	%
$\text{SOC}^{\text{EV,min}}_t$, $\text{SOC}^{\text{EV,max}}_t$, $\delta\text{SOC}^{\text{EV}}_t$	20, 90, 5	%
$P^{\text{BS}}_{\text{Charge}}$, $P^{\text{BS}}_{\text{Discharge}}$	9.3, 12.4	kW
$P^{\text{EV}}_{\text{Charge}}$, $P^{\text{EV}}_{\text{Discharge}}$	1.7, 3.5	kW
Switching frequency	20	kHz
Power grid frequency	50	Hz

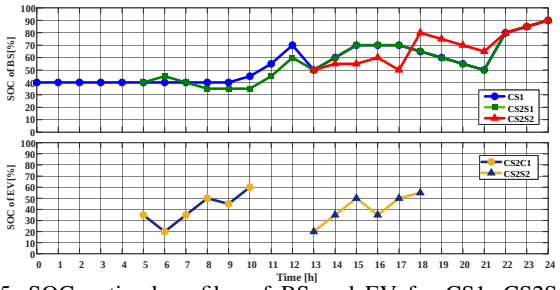

Fig. 5: SOC optimal profiles of BS and EV for CS1, CS2S1, and CS2S2

$$20\% \leq SOC^{EV}_{t_{in}} \leq 50\% \tag{18}$$

$$40\% \leq SOC^{EV}_{t_{out}} \leq 90\% \tag{19}$$

$$00{:}00 \leq t^{EV}_{in} \leq 22{:}00 \tag{20}$$

$$t^{EV}_{in} \leq t^{EV}_{out} \leq 24{:}00 \tag{21}$$

As shown in Fig. 5, the BS charge and discharge scheduling are determined based on the results obtained at time-step 00:00 (CS1). At 05:00, the system specifies the charge and discharge scheduling of both EV and BS at the same time for 10:00 and 24:00 (CS2S1), respectively. Similarly, by reconnecting the EV at 13:00, the algorithm is run again and updates the charge and discharge schedules of EV and BS for 18:00 and 24:00 (CS2S2), respectively. Therefore, SOC profile of BS with two-time random re-connection of EV follows the blue curve by 05:00. At the time interval of 05:00 to 13:00, it changes according to the green curve and for hours-ahead, it matches the red curve changes. Further, Fig. 5 shows the SOC profile of EV. Refer to this figure, not only EV is not charged at a fixed rate, but also it operates three times in V2H mode. This indicates how much EV is flexible to take part achieving problem objective.

In the case of disconnecting EV before the pre-defined time, $t^{\text{EV}}_{\text{out}}$, the proposed HEMS should be run to deal with the stochastic variation effects of the EV on the BS charge scheduling. To do this, the EV's parameters are determined randomly with the disconnection time-step, which randomly changes between $t^{\text{EV}}_{\text{in}}$ and $t^{\text{EV}}_{\text{out}}$. In this regard, at a time-step before $t^{\text{EV}}_{\text{out}}$, EV is suddenly disconnected. This is modeled by defining a flag that indicates whether EV is connected or disconnected. The number of flags is multiplied by EV power in Eq. (9). Therefore, EV disconnection leads to a change in the amount of power excess/ shortage of HEH, the weight of the remaining paths, and the optimal BS profile changes, subsequently. If EV is disconnected at a moment between two consecutive time-steps, the algorithm works based on the last scheduling until the start of the next time-step. Then, it acts as described above. In order to minimize the fluctuations of such possible problems, shorter time-steps could be applied, which is not needed in the application of this article according to the problem objectives. However, results of sudden disconnection before $t^{\text{EV}}_{\text{out}}$ for 1-hour time-steps is shown in Fig. 6. As presents

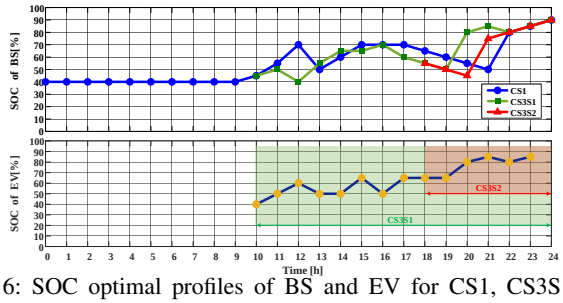

Fig. 6: SOC optimal profiles of BS and EV for CS1, CS3S1, and CS3S2

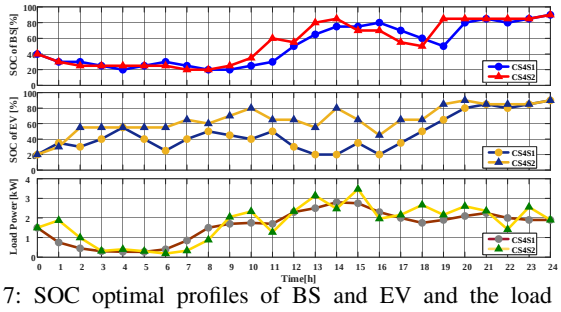

Fig. 7: SOC optimal profiles of BS and EV and the load power profiles for CS4

in this figure for EV, the green area corresponds to case that its connection/ disconnection time-steps are determined according to the random approach (CS3S1). Previously, these random parameters are presented in the definition of CS3. However, with the sudden departure of EV at 18:00, its SOC does not follow the last path obtained any more (CS3S2). Hence, SOC changes depicted in the red zone are not followed by EV and as a result, SOC of the EV does not reach the specified target value. Further, the corresponding changes of BS's SOC are shown in this figure. Therefore, BS follows the blue, green, and red curves under the sudden disconnection of the EV at intervals of 00:00-10:00, 10:00-18:00, and 18:00-24:00, respectively.

Showing the proposed algorithm capabilities in considering the possible uncertainties, Fig. 7 presents the load uncertainty (CS4) in which load power value will change randomly per step-times in a range up to $\pm 40\%$ compared to the pre-defined value. To do this, EV is connected at t_0 and the value of next time-step load power is selected randomly in the aforementioned range. The proposed algorithm is run at each time-step, considering the worst case. Therefore, at each time-step, the battery charging/ discharging scheduling is done for hours-ahead. In this regard, $\mathrm{SOC}^{BS}_{t_0+\Delta t}$ of time-step t is set as the $\mathrm{SOC}^{BS}_{t_0}$ of time-step $t+\Delta t$.

Table III compares daily purchased power price of HEH between the proposed and uncontrolled charging methods. In uncontrolled charging method, EV get charged at maximum rate whenever the EV is connected. In order to be a credible comparison, the EV's initial and target SOCs in uncontrolled charging method are equal to the corresponding previous scenarios. According to Table III, the cost of a given purchased power under the proposed control is lower than uncontrolled method.

Table IV presents the BFMA running time for different CSs. As can be seen, the data would be increased for CSs with higher number of nodes and edges. In this case, most of the time is spent creating the weight matrix. Due to the constraints shown in Fig. 4, the dimensions of the weight matrix are reduced considerably because many edges could be nullified, since the specified conditions have not been met. On the other hand, once the graph is formed, it only takes a fraction of a seconds to find the shortest path by specifying any initial and target nodes. Although, it takes maximum 1.4 s to create the graph for an HEH with a BS and an EV, the graph could be used for routing the shortest paths in future scenarios while they may take time about 0.01 s. However, the focus of this paper is on home applications, even if it develops to a multi-scheduling scheme, it still does not need to be faster [49]. A graph related to the presence of an EV is also formed at the beginning of the test to enhance the data processing speed in the practical tests. Then, the algorithm calls only the graph at the moment of random connection of EV. For applications with a couple of plugged-in EVs such as charging stations, parking, and shopping centers, artificial intelligence methods could use to train the system to achieve a higher number of nullified edges.

B. Experimental Results

The proposed two-level HEMS is implemented on a scaled-down testbed shown in Fig. 8. A DSP TMS320F28335 processor from Texas Instruments® has used to implement the proposed algorithm. Two batteries act as BS and EV, and a DC voltage source is replaced with PV. The power grid voltage is reduced through an auto-transformer and then, passed through a 1:1 isolation transformer. A current source converter with an output resistive load is utilized to emulate the controllable DC load. Thus, the amplitude of the load current in each time-step could be changed during the experimental tests. The load current profile is shown in the following changing in range from almost zero to -3 A. The system specifications are given in Table V. In the following, the performance of the proposed algorithm under experimental CSs (ECS) is verified. In the assessments, BS's and EV's currents under different ECSs are shown, which are considered as the criteria for evaluation of the effects of stochastic behavior of EV on BS current profile.

Therefore, an ECS without the presence of EV (ECS1), with the PV and load current profiles are depicted together for twenty time-steps. The i_{pv} and i_{load}, shown in Fig. 9,

TABLE III: Simulation results

Quantities	ΔP^{HEH} (kWh)	HEH purchased power price (£)	
		Proposed method	Uncontrolled charging
CS2S2	-26.77	1.5631	1.6701
CS3S2	-22.7	1.122	1.5074
CS4S2	-27.94	1.5524	1.7657

TABLE IV: Algorithm specification

Scenario	Number of nodes	Total number of edges	Nullifying percentage (%)	Number of remaining edges	Time to once forming of graph (s)
CS1	347	4980	30	3485	0.01
CS2S1	1112	158415	62	60198	0.26
CS2S2	992	156615	62.4	58887	0.22
CS3S1	2717	560490	63	207380	0.8
CS3S2	1667	308490	62.6	115380	0.52
CS4	5177	1114200	62.8	414480	1.4

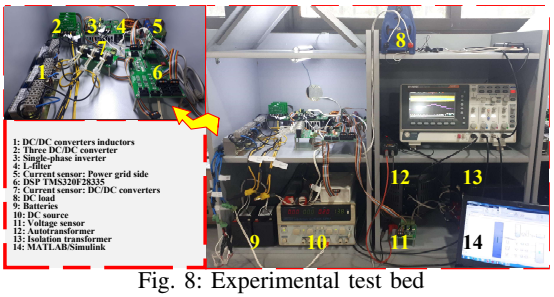

Fig. 8: Experimental test bed

are used for all ECSs. The PV generated current and the load consumption current are depicted positive and negative, respectively. The i_{BS} and i_{EV} are also obtained under following ECSs:

1) ECS1: EV is not connected and SOC_0^{BS}= 45%, and $\text{SOC}_{\text{Target}}^{\text{BS}}$= 90%.
2) ECS2: EV is connected and disconnected at two random time-steps emulating stochastic behavior of the EV. BS parameters are same as ECS1.
3) ECS3: EV is connected and disconnected at two random time-steps different from CS2 ones (ECS3S1), but it is suddenly disconnected manually (ECS3S2). Similarly, BS parameters in both CS3S1 and CS3S2 are same as ECS1.
4) ECS4: EV is connected all the time (ECS4S1). In this situation, the load uncertainty is considered (ECS4S2). Consequently, BS parameters in both CS3S1 and CS3S2 are same as ECS1.

Since, the tests are performed in a short period of time and SOC changes are negligible during this period, SOC of batteries are not measured at the time-step of EV connection and applied randomly in the algorithm. As shown in Fig. 9, the BS optimal current profile is included in several charge and discharge modes to achieve the least purchased power price. The BS current is displayed as positive and negative in charge and discharge modes, respectively. It is clear that these modes have different rates, proportional to $\delta\text{SOC}_t^{\text{BS}}$ and limited to $P_{\text{Charge}}^{\text{BS||EV}}$, $P_{\text{Discharge}}^{\text{BS||EV}}$.

With the random entry of EV in ECS2, changes are appeared on SOC of BS. By comparing Fig. 9 and Fig. 10, it can be identified that the modes and rates of sometime-steps in ECS2 are different from the responding time-steps in ECS1. Fig. 10 also represents the voltage and current on the AC side in ECS2S2. The current amplitude fluctuates with the demand of the HEH during test period. Also, the 180 degrees phase difference between voltage and current means the HEH is selling the power excess to the power grid. Similarly, ECS3S1 was tested with different initial and target conditions than ECS2. Thereafter, ECS3S1 runs again, where

TABLE V: Experimental setup specifications

Condition	Value	Unit
DC bus voltage	36	V
RMS voltage of power grid	28	V
BS and EV voltage	12	V
BS and EV capacity	7	Ah
DC source voltage (max) and current (max)	30, 3	V, A
$P_{\text{Charge}}^{\text{BS}}$, $P_{\text{Discharge}}^{\text{BS}}$	17, 17	W
$P_{\text{Charge}}^{\text{EV}}$, $P_{\text{Discharge}}^{\text{EV}}$	17, 17	W
DC/ DC converters switching frequency	40	kHz
Inverter switching frequency	3	kHz
Power grid frequency	50	Hz

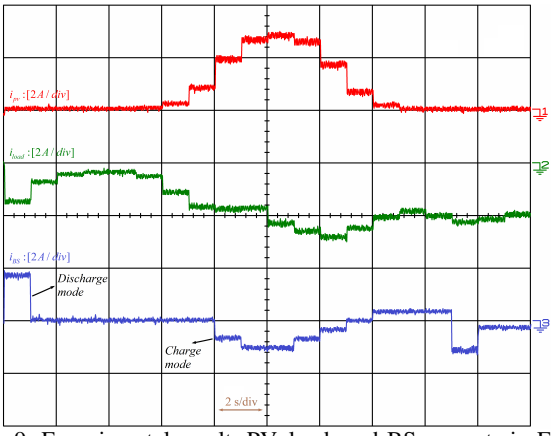

Fig. 9: Experimental result: PV, load, and BS currents in ECS1

the EV was manually disconnected before being unplugged by the algorithm (ECS3S2). Fig. 11 shows the BS's and EV's currents under these two scenarios. By comparing BS current in Fig. 9 and Fig. 11a, the effect of the presence of EV on the optimal charge and discharge profile of the BS is clear. Consequently, the sudden disconnection of EV also affects this optimal profile, as presents in Fig. 11b with a dashed ellipse. Moreover, in CS3S2, after the sudden disconnection of EV, the new optimal BS profile is applied to the system at the beginning of the next time-step because the disconnection occurred at a moment between two consecutive time-steps while the algorithm waits for run until the next time-step.

Fig. 12 illustrates the performance of the system under load uncertainty. In this test, each time-step takes 5 s for the algorithm to have sufficient time to analyze under conditions of load uncertainty. Random load changes are shown in Fig. 12b by the dashed line ellipse. The algorithm starts working as soon as the uncertainty is detected (I). During this period, the BS and EV currents have the values obtained from the previous analysis. Then, the optimal charging and discharging schedule is modified for the current and the remaining time-steps (II). Similarly, by detecting subsequent uncertainties, this procedure has repeated for intervals [III, IV], [V, VI], and [VII, VIII] leading to modifications on the optimal profile of BS's and EV's currents.

Fig. 13 represents the BS's SOC in different ECSs. This result is obtained by $SOC_0^{\text{BS}} - \frac{1}{C_{AH}^{\text{BS}}} \int i_{BS} dt$ during a 100 s time period with five-second time-steps. As mentioned above, the five-second time-steps is selected to facilitate enough time to the algorithm to perform analysis in case of load uncertainty. As can be seen, the effect of stochastic behavior of EV and load uncertainty on BS' SOC is proportion to associated currents.

V. Conclusion

This study has developed a smart charging solution for EVs and provided a practical implementation for domestic applications. In this respect, a two-level HEMS has been proposed where the modified BFMA has been included at the secondary level for optimal charging the EV and BS. Furthermore, the proposed HEMS is suitable for real-time decision making in the multi-energy systems where the optimal profile of charge/ discharge in batteries (BSs and EVs) could be evaluated by the user profitability. Eventually,

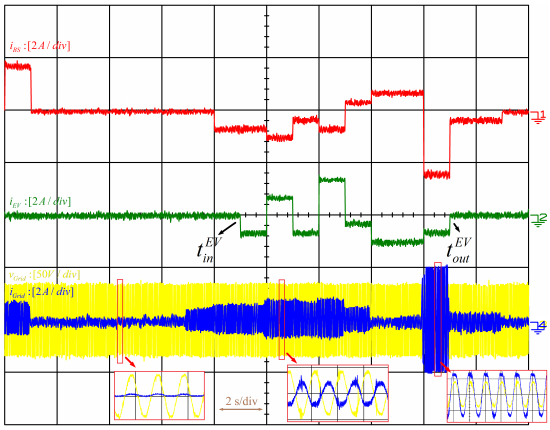

Fig. 10: Experimental result: BS an EV currents in ECS2

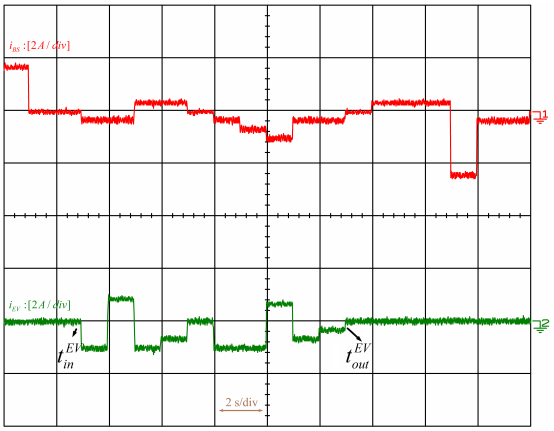

(a) CS3S1

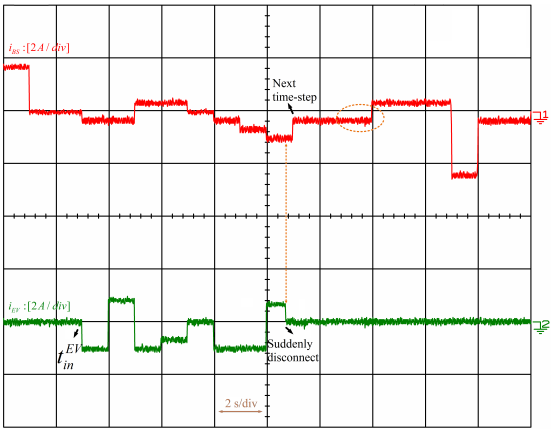

(b) CS3S2

Fig. 11: Experimental result: BS and EV currents in ECS3

the performance of the proposed HEMS has been practically validated by a testbed accompanied with a DC-source, BS, and EV connected to the power grid.

REFERENCES

[1] J. A. Sanguesa, V. Torres-Sanz, P. Garrido, F. J. Martinez, and J. M. Marquez-Barja, "A review on electric vehicles: Technologies and challenges," *Smart Cities*, vol. 4, no. 1, pp. 372–404, 2021.

[2] M. Yousefi, A. Hajizadeh, M. N. Soltani, and B. Hredzak, "Predictive home energy management system with photovoltaic array, heat pump, and plug-in electric vehicle," *IEEE Transactions on Industrial Informatics*, vol. 17, no. 1, pp. 430–440, 2020.

[3] A. Elmouatamid, R. Ouladsine, M. Bakhouya, N. El Kamoun, M. Khaidar, and K. Zine-Dine, "Review of control and energy management approaches in micro-grid systems," *Energies*, vol. 14, no. 1, p. 168, 2021.

[4] H. R. Gholinejad, J. Adabi, and M. Marzband, "An energy management system structure for neighborhood networks," *Journal of Building Engineering*, p. 102376, 2021.

[5] N. D. Van, M. Sualeh, D. Kim, and G.-W. Kim, "A hierarchical control system for autonomous driving towards urban challenges," *Applied Sciences*, vol. 10, no. 10, p. 3543, 2020.

[6] Y. Luo, X. Zhang, D. Yang, and Q. Sun, "Emission trading based optimal scheduling strategy of energy hub with energy storage and integrated electric vehicles," *Journal of Modern Power Systems and Clean Energy*, vol. 8, no. 2, pp. 267–275, 2020.

[7] K. Mahmud, M. S. H. Nizami, J. Ravishankar, M. J. Hossain, and P. Siano, "Multiple home-to-home energy transactions for peak load shaving," *IEEE Transactions on Industry Applications*, vol. 56, no. 2, pp. 1074–1085, 2020.

[8] Y. Xiang, Y. Wang, S. Xia, and F. Teng, "Charging load pattern extraction for residential electric vehicles: A training-free non-intrusive method," *IEEE Transactions on Industrial Informatics*, 2021.

[9] S. Paul and N. P. Padhy, "Resilient scheduling portfolio of residential devices and plug-in electric vehicle by minimizing conditional value at risk," *IEEE Transactions on Industrial Informatics*, vol. 15, no. 3, pp. 1566–1578, 2018.

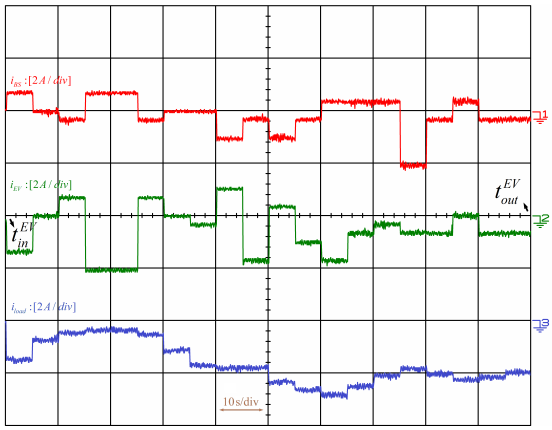

(a) CS4S1

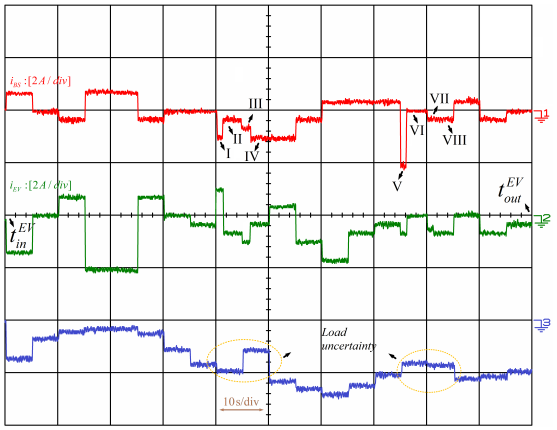

(b) CS4S2

Fig. 12: Experimental result: BS and EV currents in ECS4

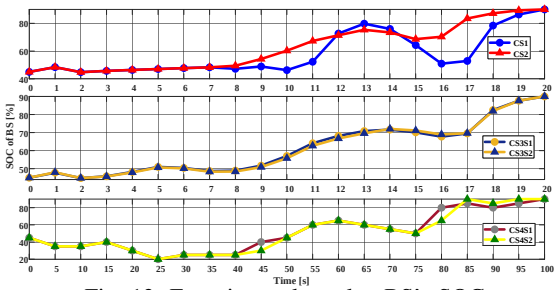

Fig. 13: Experimental results: BS's SOC

[10] A. Verma, B. Singh, A. Chandra, and K. Al-Haddad, "An implementation of solar pv array based multifunctional ev charger," *IEEE Transactions on Industry Applications*, vol. 56, no. 4, pp. 4166–4178, 2020.

[11] Z. Zhao and C. Keerthisinghe, "A fast and optimal smart home energy management system: State-space approximate dynamic programming," *IEEE Access*, vol. 8, pp. 184 151–184 159, 2020.

[12] F. Morlock, B. Rolle, M. Bauer, and O. Sawodny, "Time optimal routing of electric vehicles under consideration of available charging infrastructure and a detailed consumption model," *IEEE Transactions on Intelligent Transportation Systems*, vol. 21, no. 12, pp. 5123–5135, 2019.

[13] R. Rana, S. Prakash, and S. Mishra, "Energy management of electric vehicle integrated home in a time-of-day regime," *IEEE Transactions on Transportation Electrification*, vol. 4, no. 3, pp. 804–816, 2018.

[14] H. Kikusato, K. Mori, S. Yoshizawa, Y. Fujimoto, H. Asano, Y. Hayashi, A. Kawashima, S. Inagaki, and T. Suzuki, "Electric vehicle charge–discharge management for utilization of photovoltaic by coordination between home and grid energy management systems," *IEEE Transactions on Smart Grid*, vol. 10, no. 3, pp. 3186–3197, 2018.

[15] E. Shirazi and S. Jadid, "Optimal residential appliance scheduling under dynamic pricing scheme via hemdas," *Energy and Buildings*, vol. 93, pp. 40–49, 2015.

[16] X. Hou, J. Wang, T. Huang, T. Wang, and P. Wang, "Smart home energy management optimization method considering energy storage and electric vehicle," *IEEE Access*, vol. 7, pp. 144 010–144 020, 2019.

[17] G. Abdelaal, M. I. Gilany, M. Elshahed, H. M. Sharaf *et al.*, "Integration of electric vehicles in home energy management considering urgent charging and battery degradation," *IEEE Access*, vol. 9, pp. 47 713–47 730, 2021.

[18] N. Bodenschatz, M. Eider, and A. Berl, "Mixed-integer-linear-programming model for the charging scheduling of electric vehicle fleets," in *2020 10th International Conference on Advanced Computer Information Technologies (ACIT)*. IEEE, 2020, pp. 741–746.

[19] A. Mansour-Saatloo, Y. Pezhmani, M. A. Mirzaei, B. Mohammadi-Ivatloo, K. Zare, M. Marzband, and A. Anvari-Moghaddam, "Robust decentralized optimization of multi-microgrids integrated with power-to-x technologies," *Applied Energy*, vol. 304, p. 117635, 2021.

[20] A. C. Luna, N. L. Diaz, M. Graells, J. C. Vasquez, and J. M. Guerrero, "Mixed-integer-linear-programming-based energy management system for hybrid pv-wind-battery microgrids: Modeling, design, and experimental verification," *IEEE Transactions on Power Electronics*, vol. 32, no. 4, pp. 2769–2783, 2016.

[21] M. O. Badawy and Y. Sozer, "Power flow management of a grid tied pv-battery system for electric vehicles charging," *IEEE Transactions on Industry Applications*, vol. 53, no. 2, pp. 1347–1357, 2016.

[22] A. S. Bouhouras, P. A. Gkaidatzis, I. Panapakidis, A. Tsiakalos, D. P. Labridis, and G. C. Christoforidis, "A pso based optimal evs charging utilizing besss and pvs in buildings," pp. 1–6, 2019.

[23] T. He, M. Wu, D. D.-C. Lu, R. P. Aguilera, J. Zhang, and J. Zhu, "Designed dynamic reference with model predictive control for bidirectional ev chargers," *IEEE Access*, vol. 7, pp. 129 362–129 375, 2019.

[24] R. Wang, G. Xiao, and P. Wang, "Hybrid centralized-decentralized (hcd) charging control of electric vehicles," *IEEE Transactions on Vehicular Technology*, vol. 66, no. 8, pp. 6728–6741, 2017.

[25] Q. Chen, N. Liu, X. Lu, and J. Zhang, "A heuristic charging strategy for real-time operation of pv-based charging station for electric vehicles," pp. 465–469, 2014.

[26] S. Zhao, X. Lin, and M. Chen, "Robust online algorithms for peak-minimizing ev charging under multistage uncertainty," *IEEE Transactions on Automatic Control*, vol. 62, no. 11, pp. 5739–5754, 2017.

[27] A. Shahkamrani, H. Askarian-abyaneh, H. Nafisi, and M. Marzband, "A framework for day-ahead optimal charging scheduling of electric vehicles providing route mapping: Kowloon case study," *Journal of Cleaner Production*, vol. 307, p. 127297, 2021.

[28] J. A. A. Silva, J. C. López, N. B. Arias, M. J. Rider, and L. C. da Silva, "An optimal stochastic energy management system for resilient microgrids," *Applied Energy*, vol. 300, p. 117435, 2021.

[29] S. Zeynali, N. Nasiri, M. Marzband, and S. N. Ravadanegh, "A hybrid robust-stochastic framework for strategic scheduling of integrated wind farm and plug-in hybrid electric vehicle fleets," *Applied Energy*, vol. 300, p. 117432, 2021.

[30] S. Wang, H. Gangammanavar, S. D. Ekşioğlu, and S. J. Mason, "Stochastic optimization for energy management in power systems with multiple microgrids," *IEEE Transactions on Smart Grid*, vol. 10, no. 1, pp. 1068–1079, 2017.

[31] S. M. Kazemi-Razi, H. Askarian Abyaneh, H. Nafisi, Z. Ali, and M. Marzband, "Enhancement of flexibility in multi-energy microgrids considering voltage and congestion improvement: Robust thermal comfort against reserve calls," *Sustainable Cities and Society*, vol. 74, p. 103160, 2021.

[32] B. Faridpak, M. Farrokhifar, A. Alahyari, and M. Marzband, "A mixed epistemic-aleatory stochastic framework for the optimal operation of hybrid fuel stations," *IEEE Transactions on Vehicular Technology*, vol. 70, no. 10, pp. 9764–9774, 2021.

[33] S. Aznavi, P. Fajri, A. Asrari, and F. Harirchi, "Realistic and intelligent management of connected storage devices in future smart homes considering energy price tag," *IEEE Transactions on Industry Applications*, vol. 56, no. 2, pp. 1679–1689, 2019.

[34] M. S. Jonban, L. Romeral, A. Akbarimajd, Z. Ali, S. S. Ghazimirsaeid, M. Marzband, and G. Putrus, "Autonomous energy management system with self-healing capabilities for green buildings (microgrids)," *Journal of Building Engineering*, vol. 34, p. 101604, 2021.

[35] M. J. Sanjari, H. Karami, and H. B. Gooi, "Analytical rule-based approach to online optimal control of smart residential energy system," *IEEE Transactions on Industrial Informatics*, vol. 13, no. 4, pp. 1586–1597, 2017.

[36] H. Li, Z. Wan, and H. He, "Constrained ev charging scheduling based on safe deep reinforcement learning," *IEEE Transactions on Smart Grid*, vol. 11, no. 3, pp. 2427–2439, 2019.

[37] A. K. Masih and H. Verma, "Management of battery using ann controller for renewable hybrid system," pp. 1–6, 2021.

[38] N. Gholizadeh, M. Abedi, H. Nafisi, M. Marzband, A. Loni, and G. A. Putrus, "Fair-optimal bilevel transactive energy management for community of microgrids," *IEEE Systems Journal*, pp. 1–11, 2021.

[39] F. Berthold, A. Ravey, B. Blunier, D. Bouquain, S. Williamson, and A. Miraoui, "Design and development of a smart control strategy for plug-in hybrid vehicles including vehicle-to-home functionality," *IEEE Transactions on Transportation Electrification*, vol. 1, no. 2, pp. 168–177, 2015.

[40] A. Eajal, M. F. Shaaban, E. El-Saadany, and K. Ponnambalam, "Fuzzy logic-based charging strategy for electric vehicles plugged into a smart grid," *International Journal of Process Systems Engineering*, vol. 4, no. 2-3, pp. 119–137, 2017.

[41] K. K. Jaladi, S. Kumar, and L. M. Saini, "Anfis controlled grid connected electric vehicle charging station using pv source," pp. 1–5, 2020.

[42] P. García, C. A. García, L. M. Fernández, F. Llorens, and F. Jurado, "Anfis-based control of a grid-connected hybrid system integrating renewable energies, hydrogen and batteries," *IEEE Transactions on industrial informatics*, vol. 10, no. 2, pp. 1107–1117, 2013.

[43] L. N. An and T. Q. Tuan, "Dynamic programming for optimal energy management of hybrid wind–pv–diesel–battery," *Energies*, vol. 11, no. 11, p. 3039, 2018.

[44] Z. Zhao and C. Keerthisinghe, "A fast and optimal smart home energy management system: State-space approximate dynamic programming," *IEEE Access*, vol. 8, pp. 184 151–184 159, 2020.

[45] C. Papadimitriou, E. Zountouridou, and N. Hatziargyriou, "Review of hierarchical control in dc microgrids," *Electric Power Systems Research*, vol. 122, pp. 159–167, 2015.

[46] J. A. Cortajarena, O. Barambones, P. Alkorta, and J. De Marcos, "Sliding mode control of grid-tied single-phase inverter in a photovoltaic mppt application," *Solar Energy*, vol. 155, pp. 793–804, 2017.

[47] B. Jeddi, Y. Mishra, and G. Ledwich, "Differential dynamic programming based home energy management scheduler," *IEEE Transactions on Sustainable Energy*, vol. 11, no. 3, pp. 1427–1437, 2019.

[48] J. Y. Yong, V. K. Ramachandaramurthy, K. M. Tan, and J. Selvaraj, "Experimental validation of a three-phase off-board electric vehicle charger with new power grid voltage control," *IEEE Transactions on Smart Grid*, vol. 9, no. 4, pp. 2703–2713, 2016.

[49] X. Jin, J. Wu, Y. Mu, M. Wang, X. Xu, and H. Jia, "Hierarchical microgrid energy management in an office building," *Applied Energy*, vol. 208, pp. 480–494, 2017.